PHYSICAL REVIEW C VOLUME 22, NUMBER 3 SEPTEMBER 1980

Light-charged-particle emission in ^{40}Ar-induced reactions: A probe of the very early evolution of the collisions

D. Logan
Department of Chemistry, Carnegie-Mellon University, Pittsburgh, Pennsylvania 15213

H. Delagrange,* M. F. Rivet,† M. Rajagopalan, and John M. Alexander
Department of Chemistry, State University of New York at Stony Brook, Stony Brook, New York 11794

Morton Kaplan
Department of Chemistry, Carnegie-Mellon University, Pittsburgh, Pennsylvania 15213

M. S. Zisman
Lawrence Berkeley Laboratory, Berkeley, California 94720

E. Duek
Department of Chemistry, State University of New York at Stony Brook, Stony Brook, New York 11794
(Received 11 March 1980)

Charged-particle emission was studied for the reactions 222, 274, and 340 MeV ^{40}Ar+^{116}Sn, ^{154}Sm, ^{164}Dy, and ^{197}Au. Energy and angular distributions were measured for H and He and angular distributions for Li, Be, B, C, N, and O, fissionlike fragments and evaporation residues. For H and He the data are consistent with a low-temperature evaporative component and a high-temperature forward peaked component. For Li through O the forward-peaked emission was studied for 340 MeV ^{40}Ar only. The evaporation residue cross sections decrease strongly with increasing Z reflecting the increasing fissionability. However, the cross sections for ^{1}H and ^{4}He in coincidence with fission are essentially constant with Z. Coincidence measurements, energy spectra, and ^{4}He/^{1}H ratios indicate that most H/He evaporation precedes fission. This implies that the energy thermalization is very rapid indeed and that the light particle spectra can probe the very early history of the composite systems.

[NUCLEAR REACTIONS ^{116}Sn, ^{154}Sm, ^{164}Dy, ^{197}Au (^{40}Ar; H/He, fission and evaporation residues), E=222, 274, and 340 MeV, measured energy and angular distributions in singles mode. For E=340 MeV, coincidence measurements between H/He and one fission-like fragment, and angular distributions for Li, Be, B, C, N, and O in the singles mode.]

I. INTRODUCTION

This paper is one of a series in which we study heavy-ion reactions by measurements of the light-charged particles (H/He) along with the heavier fragments such as evaporation residues (ER) and fission fragments.[1-4] Our emphasis here is on the attempt to form various compound nuclei $^{156}_{68}$Er, $^{194}_{80}$Hg, $^{204}_{84}$Po, and $^{237}_{97}$Bk at excitation energies up to 200 MeV and spins of a hundred or so. At these very high energies the concept of "fusion" is complicated by the occurrence of complete and partial or incomplete fusion and by the similarities of "true fission" and "fission-like" reactions.[2,3] These complications impinge on the utility of the oft-used sharp-cutoff approximation for l_{crit}, the critical l value for fusion. Nevertheless we try to extract fusion cross sections, l_{crit} values, and the temperatures of the composite nuclei. The thermometer we use is the high-energy part of the H/He spectra at backward angles.[5,6] Evidence is presented that much H/He evaporation precedes fission; therefore, the maximum and the low-energy part of the evaporation spectra reflect the Coulomb barriers of the newly born composite nuclei and thus give some ideas on their shapes or identities.[7] The competition between fission and particle evaporation is reflected by the relative cross sections for H/He, ER, and fission. The importance and the nature of direct H/He emission is viewed by the angular and energy distributions, particularly at forward angles.[5,6] In other papers[1,4] we have explored in a similar manner the energy and spin dependence of deexcitation of ^{194}Hg and ^{156}Er. Also, we have presented in Ref. 2 a somewhat more detailed study of one reaction, 340 MeV ^{40}Ar +^{197}Au.

In 1961 Britt and Quinton showed that both direct and evaporative components could be identified in H/He spectra from reactions between complex nuclei.[5] Galin *et al.*[8] demonstrated for the composite

system ^{117}Te that the direct components were much less important for ^{40}Ar than for ^{14}N induced reactions (excitations of 71 and 107 MeV), and this suggested ^{40}Ar (or similar projectiles) as particularly useful for producing compound nuclei after complete fusion. The preponderance of deeply inelastic collisions for even heavier projectiles, for example ^{86}Kr, also argues for ^{40}Ar as a good choice of projectile for systematic studies of compound nuclei.[9]

Fusion cross section measurements at low energies make it possible to estimate the fusion barriers.[10-14] These barriers and semiempirical theories allow estimates of the critical l values for fusion. Recently the evidence has been mounting that forward peaked ^{4}He emission is often correlated with *partial* fusion reactions[2,15-19] rather than projectile breakup,[5] and thus the notion of straightforward identification of "evaporation residues" after truly complete fusion has been put in question.[3] One of our objectives in this study is to determine the magnitude of such forward-peaked H/He particles and therefore their possible influence on the concept of complete fusion and l_{crit}.[20] A preliminary discussion of this question has already been published.[3]

To the extent that "complete (and incomplete) fusion" can be identified, we seek its dependence on target and energy. Particle evaporation has been shown to precede fission in substantial amounts[2] for 340 MeV ^{40}Ar + ^{197}Au. Here we seek the Z dependence of this fission-evaporation competition. Standard parametrizations of the statistical model indicate that with increasing energy, charge, and spin, fission should increasingly dominate H/He emission from an equilibrated system.[21] The experimental data seem to be inconsistent with this prediction of the equilibrium statistical model. Thus we feel that the whole question of energy equilibration and the power of "available phase space" as a driving force must be studied by systematic experimentation for nuclei at high excitation and spin.

In Sec. II we sketch the experimental techniques and in Sec. III we present the results. Some of the relationships to earlier experiments and simple reaction models are discussed along with the data presentation. In Sec. IV we set some time limits on the decay of composite systems prior to equilibration. We discuss the spin zones for fission and evaporation and some misleading features of "sharp-cutoff" thinking. Evidence is presented for the breakdown of phase-space equations for fission-evaporation competition in reactions of 340 MeV ^{40}Ar. Finally a flow chart of the cross sections and mean spins is presented along with some suggestions for future experimentation.

II. EXPERIMENTAL ARRANGEMENT

Beams of ^{40}Ar were provided by the SuperHILAC at the Lawrence Berkeley Laboratory. They were defined by two four-jaw collimators upstream of the 75 cm diameter scattering chamber. Self-supporting targets were used of ^{116}Sn, ^{154}Sm, ^{164}Dy, and ^{197}Au (0.85, 0.67, 1.00, and 1.25 mg/cm^2, respectively); each contained >95% of the isotope indicated. The thickness of the Au target was measured by weight and the other target thicknesses were determined relative to it by elastic scattering. The mean charge states of the beam were taken to be 16.3, 15.3, and 15.0 at 340, 274, and 222 MeV, respectively.[22] These values are consistent with the assumption of Rutherford scattering from Au at small angles. The beam intensity was limited by the dead time of the system ($\approx$ 10–20%). Elimination of the buncher was found to allow a significant increase in beam intensity, and the introduction of a new and faster ADC and multiplexer system allowed significantly higher counting rates for the last run (some of the 340 MeV data). Dead time was measured by a pulser triggered by one of two beam monitors and passed through the test input of selected preamplifiers.

The basic detection scheme has been described elsewhere[1,2,4]: gas ionization telescope (GT) ($\approx$20 Torr of methane and 300 μm Si stopping detector)[23] for ER and fission products, solid state telescope (SST) (45 μm, 500 μm, 5mm Si detectors) for light charged particles (H, He, Li, ... O) and in some cases fission products. For the SST, cover foils of either 10 or 50–70 mg/cm^2 Pb were used (the latter was chosen to stop completely the elastically scattered ^{40}Ar at the more forward angles). Normally an SST was mounted such that $\Delta\Omega \approx 8$ msr which allowed approach to about 20° from the beam axis. For the 340 MeV experiment, one SST was mounted at a much lower geometry ($\Delta\Omega \approx 0.8$ msr) which allowed measurements to be made as close as 5° to the beam. Energy calibrations and pulse height defects for the GT were made by the elastically scattered beam and by a source of ^{252}Cf; for the SST, sources of ThB were used. For light-charged particles that barely enter the third member of the SST, a small experimental problem arises. If less than $\approx$0.5 MeV is deposited in this third detector, then the processing of this pulse is nonlinear. At worst this results in the assignment of an apparent energy for this particle from only the first two members of the SST. This effect can be seen as an apparent discontinuity in the ^{4}He spectra in Figs. 1 and 2 ($\theta_{c.m.} = 6°$ and 18°). A correction could be applied by averaging the one high point for $\epsilon_{c.m.} \approx 24$ MeV with the one low point for $\epsilon_{c.m.} \approx 25$ MeV. We have no reason to believe that

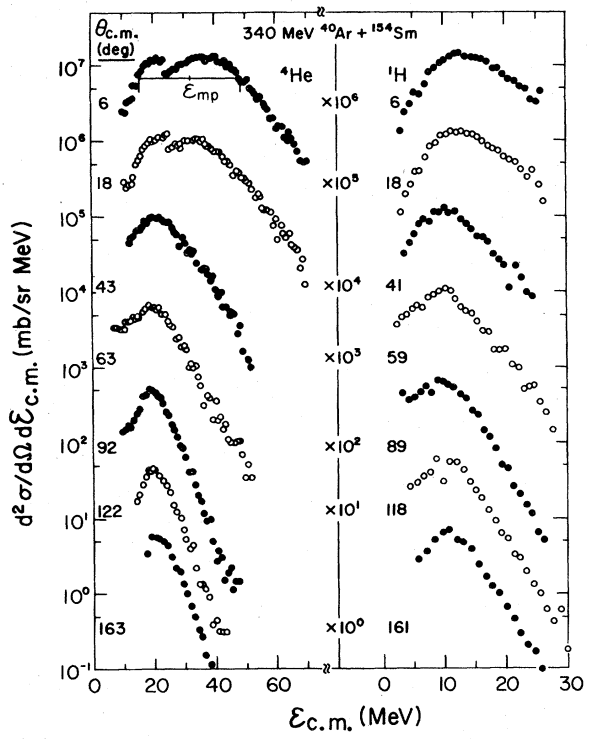

FIG. 1. Singles energy spectra (c.m.) for ^{4}He and ^{1}H at various angles. The average c.m. angle is indicated and the corresponding multiplier is on the same horizontal line. Parameters describing the spectra are given in Table I, and one indication is shown for ϵ_{mp}.

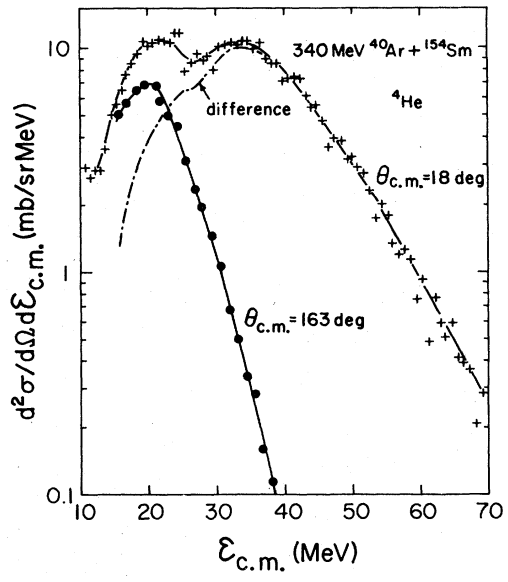

FIG. 2. Spectra for ^{4}He at a forward and a backward angle and their difference.

the spectra are distorted outside this very narrow zone.

One set of measurements was made for coincidence between fission and H/He (emitted in the backward direction) from 340 MeV ^{40}Ar + ^{116}Sn, ^{154}Sm, and ^{164}Dy. Similar measurements had already been made[2] for ^{197}Au. Fission fragments were recorded in the GT at $\Delta\Omega \approx 1$ msr and $\theta_{lab} \approx 51°$ ($\theta_{c.m.} \approx 90°$); and H/He were recorded at θ_{lab} of 79°, 104°, and 129° ($\theta_{c.m.} \approx 90°$, 120°, and 140°) in the reaction plane. A time to amplitude converter (TAC) was used to record the spectrum of time delays between pulses from the GT and SST. This spectrum gave a true coincidence peak of about 30 nsec width and a small flat tail indicating a negligible rate of random coincidences. Single events were prescaled by a factor of 100 and recorded simultaneously with the coincident events. One set of measurements was also made (340 MeV ^{40}Ar beam) of Li, Be, B, C, N, and O at lab angles from 6–40°. Energy thresholds for these particles of Z(3–8) were rather high and thus we could observe them only at forward angles.

III. EXPERIMENTAL RESULTS

A. Qualitative features

The overall features of the energy and angular distributions in the singles mode are illustrated in Figs. 1–4 and in Table I. For $\theta_{c.m.} \gtrsim 40°$ the spectra exhibit one broad peak and an exponential high-energy tail that depends on angle (Fig. 1). For the smallest angles the spectra often break into two components. The low-energy peak is of similar energy to that observed at large angles while the high-energy component is much broader as shown in Fig. 2. If one assumes that an evaporative component is present then it can be identified with the observed spectra at backward angles. The subtraction of this component from the observed spectra at forward angles can expose the spectra from direct processes (see Fig. 2);[6] they are very broad with no obvious connection to the beam velocity. The energies and the cross sections decrease rapidly with increasing angle as shown in Figs. 1 and 3. The characteristics of this direct component will be discussed later in Sec. IV and in more detail in future publications.

In Table I we characterize the shapes of these c.m. spectra by three parameters, the full width at half maximum (FWHM), the mid point of this width (ϵ_{mp}), and the temperature (T). The latter is obtained by fitting to the function

$$P(\epsilon) \propto (\epsilon - B)\exp(-\epsilon/T) \qquad (1)$$

with the value of the barrier parameter B taken from Ref. 7. The T parameter obtained at back-

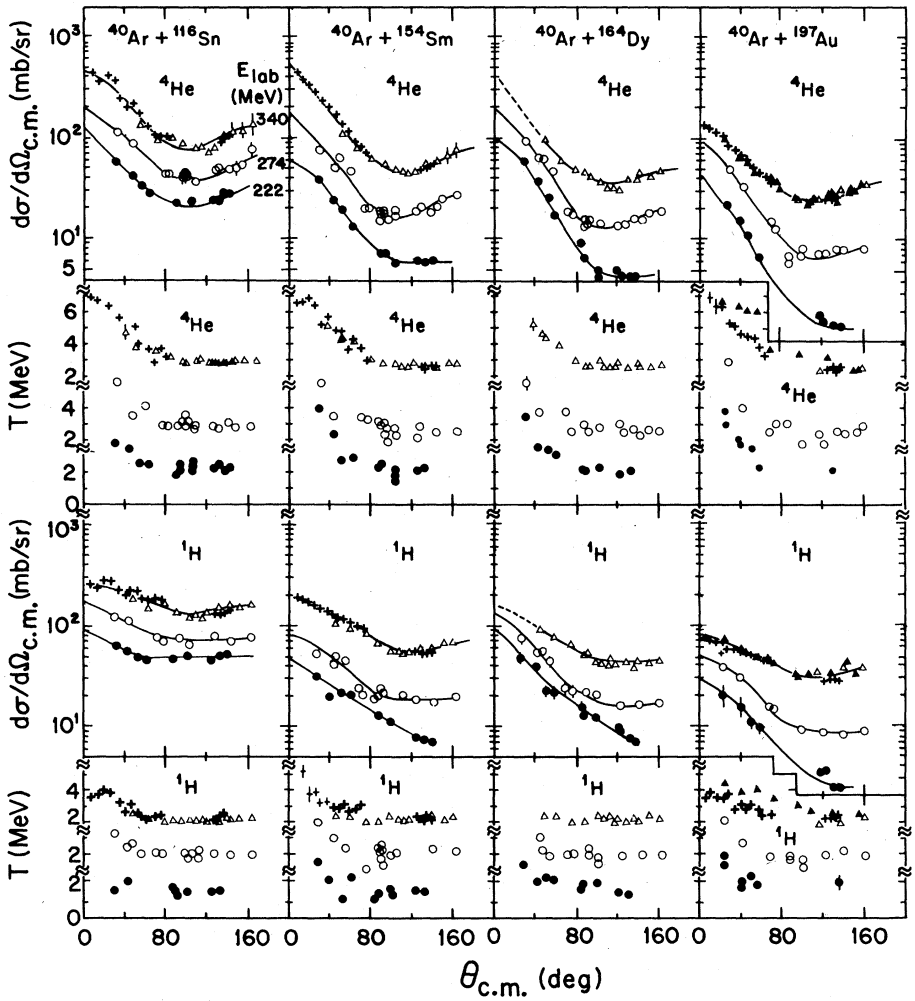

FIG. 3. Measured angular dependence of $(d\sigma/d\Omega)$ and T for ^{4}He and ^{1}H. The incident energies are indicated at the upper left. Different symbols are for different experiments; filled triangles are from Ref. 2. See Table II and its footnotes.

ward angles may be taken as a crude approximation to the nuclear temperature. For forward angles the T parameter simply gives a description of the spectral shape and has no obvious physical interpretation. The values of ϵ_{mp}, FWHM, and T are given for typical forward and backward angles of each set in Table I.

For all targets and ^{40}Ar beams of 270 and 340 MeV (Fig. 3) the spectra at back angles relax to a constant temperature with angular distribution consistent with evaporative decay (flat or slowly rising toward 180°). The magnitude and shape of the evaporative components were determined from the angular distributions for $\theta_{c.m.} > 120°$ with the assumption that the direct component vanishes beyond this angle. The energy spectra were totally relaxed in this region, and thus we have used a fitting function from the equilibrium statistical model[24,25]:

$$W(\theta_{c.m.}) = W_0 \exp[-(\beta_2/2)\sin^2\theta_{c.m.}] I_0[(\beta_2/2)\sin^2\theta_{c.m.}], \quad (2)$$

where W_0 and β_2 are free parameters and I_0 is the zeroth order modified Bessel function. The fit was made by a least squares technique using the code MINUIT. The anisotropy parameter β_2 will be related to the spins of the emitters in subsection C. After subtraction of this evaporative component (symmetric about 90°) the remaining forward-peaked (direct) component was fitted to the function

$$W(\theta) = A \exp(-b\theta - c\theta^2). \quad (3)$$

The total "evaporative" and "direct" components were determined by integration of these functions. The smooth curves in Fig. 3 show the results of the fits, and the integrated cross sections are summarized in Table II. For 222 MeV ^{40}Ar reac-

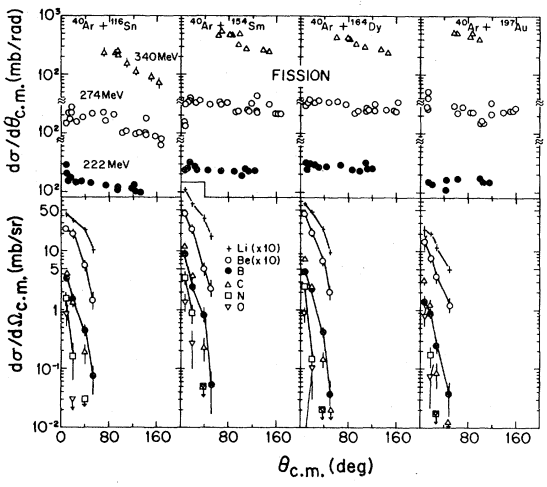

FIG. 4. Angular distributions for the fission-like products (upper) and for Li, Be, B, C, N, O (lower). Energy thresholds and integrated cross sections are given in Table II.

tions with Sm, Dy, and Au the temperature seems relaxed but the angular distributions never decisively lose their "preference" for more forward angles (for the angular range of this study). For these cases the evaporative component was assumed to be isotropic and $d\sigma/d\Omega$ was identified with the smallest measured value. Therefore these cross sections should be taken as upper limits for evaporation. By contrast, for the Sn target the evaporative component is considerably larger than the direct component. Apparently this trend continues for the even lighter target ^{77}Se as Galin *et al.*[8] observed essentially pure evaporative emission for this case. Note, however, that angles smaller than ≈20° were not explored for excitations of ≤140 MeV in either this work or in Ref. 8.

We were able to make some initial observations of Li, Be, B, C, N, and O products with the same SST and absorber foils used primarily for H/He measurements. As the energy thresholds were rather high we did not study the possibility of emission at back angles. Nevertheless these products were clearly identified at forward angles and their angular distributions and integrated cross sections are given in Fig. 4 and Table II. We have

TABLE I. Parameters that describe the energy spectra for ^{1}H and ^{4}He.

		^{4}He				^{1}H			
E_{lab} (MeV)	Target	$\theta_{c.m.}$ (deg)	ϵ_{mp} [a] (MeV)	FWHM [a] (MeV)	T (MeV)	$\theta_{c.m.}$ (deg)	ϵ_{mp} [a] (MeV)	FWHM [a] (MeV)	T (MeV)
220	^{116}Sn	142			2.09±0.05	134	8.5±1	9.2±2	1.77±0.02
		31	19.9 ±1	12.8±2	3.76±0.3	44	8.2±1	7.6±2	1.85±0.08
271		147	20.3 ±1	10 ±2	2.76±0.05	163	9.3±1	8.9±2	2.03±0.05
		32	20.2 ±1	13.3±2	5.63±0.19	30.5	8.8±1	11.5±2	3.31±0.28
339		155	19.5 ±1	9 ±1	3.04±0.11	153	9.4±0.5	8.8±0.5	2.18±0.03
		19	27.2 ±1	30 ±1	6.45±0.3	18	11.4±1	12.2±1	4.0 ±0.1
		6.5	27.5 ±1	31 ±1	7.0 ±0.2	6	11.2±0.5	12.6±1	3.56±0.15
221	^{154}Sm	135	19 ±1	10.3±2	2.29±0.30	132.5	9.3±1	9.6±2	1.75±0.30
		30	23.5 ±1	15.2±2	6.00±0.50	29	9.3±1	9.6±2	3.41±0.50
272		163	20.7 ±1	11.7±2	2.69±0.30	162	9.8±1	10.8±2	2.2 ±0.3
		30	23.5 ±1	16.6±2	5.61±0.5	29	10.3±1	10.4±2	4.0 ±0.5
340		153.5	20.35±0.5	9.3±1	2.86±0.11	151	10.5±0.5	9.8±1	2.21±0.05
		18	29.8 ±1	29.6±1	7.0 ±0.3	18	13.6±1	13.3±1	3.8 ±0.5
		6	32.5 ±1	35.0±1	6.68±0.25	6	14.1±0.5	13.8±1	4.1 ±0.2
221	^{164}Dy	134	19.3 ±1	11.4±2	2.12±0.10	133			1.57±0.11
		29	25.2 ±1	16.2±2	5.41±0.16	28	10.3±1	11.4±2	3.31±0.29
272		152	21.9 ±1	12.2±2	2.70±0.10	142	9.8±1	11 ±2	2.04±0.10
		30	25.6 ±1	16.8±2	5.66±0.30	42.8	9.1±1	12.2±2	3.13±0.36
339		153	21.2 ±0.5	10 ±1	2.57±0.10	151	9.5±0.5	10.2±0.5	2.37±0.06
		49	19.6 ±0.5	16.5±1	4.64±0.14	46	10.2±1	11.3±1	2.47±0.09
219	^{197}Au	138	21.2 ±1	15.8±2		137			2.29±0.30
		29	27.2 ±1	16.7±2	5.78±0.22	27	11.1±1	12.6±2	3.93±0.48
270		162	22.6 ±1	14.5±2	2.87±0.23	161			1.87±0.10
		29	27.3 ±1	16.4±2	6.91±0.38	28	11.2±2	12.5±3	4.05±0.22
339		150	23.0 ±1	11 ±2	2.4 ±0.2	150	12 ±1	12 ±2	2.5 ±0.2
		18	27.4 ±1	21.9±2	6.4 ±0.5	17	13.6±0.5	12.7±1	3.4 ±0.3
		6	25.4 ±1	18.6±1	8.5 ±0.5	6	12.8±0.5	13.8±1	3.55±0.11

[a] The full width at half maximum is FWHM and its midpoint is ϵ_{mp}. For those cases with no entry the spectrum did not fall to half height at low energies and therefore FWHM could not be fixed.

TABLE II. Integrated charged particle cross sections (mb).

E_{lab} (MeV)	Target	Symmetric ^{4}He	Symmetric ^{1}H	Symmetric ^{2}H	Symmetric ^{3}H	Forward peaked ^{4}He	Forward peaked ^{1}H	Forward peaked ^{2}H	Forward peaked ^{3}H
185		194	453	9.1	2.5				
220		315	628	19.7	3.7	93 [a]	31	7.1	2.1
271	^{116}Sn	555	956	57.4	17.7	228 [a]	155	21.6	7.6
339		1158	1697	155	56.6	495 [a]	466	75	21.6
221		77	73.5	6.7	2.9	83 [a]	90	8	2.3
272	^{154}Sm	232	242	31.4	15.6	195 [a]	123	18.3	7.3
340		624	703	108	66	566 [a]	392	77	36
221		56.4	91.4	4.8	2.1	151 [a]	151	14.3	3.3
272	^{164}Dy	176	205	24.7	13.7	235 [a]	190	21.8	9.5
340		478	553	83	46.5	386 [a]	251	45	26.5
219		18.8	31.7	1.7	0.90	58 [a]	54	6.6	1.4
270	^{197}Au	96	106	11.8	7.7	122 [a]	83	10.5	3.9
339 [c]		359	386	50	33	204 [a]	127	29	13
Detection threshold (MeV, lab)		8	2	3	3	14-18 [b]	3-5 [b]	5-6 [b]	6-7 [b]

		Forward peaked Li	Be	B	C	N	O
339	^{116}Sn	7.2	2.8	2.4	2.1	0.45	0.19
	^{154}Sm	11.6	2.9	4.1	4.1	1.1	0.4
	^{164}Dy	7.5	2.8	2.5	2.7	0.47	0.18
	^{197}Au	3.2	1.1	0.94	1.11	0.21	0.17
Detection threshold (MeV, lab)		36	57	78	105	125	160

[a] c.m. energy >10 MeV for Sn and >12 MeV for Sm, Dy, and Au. Substantial emission was also observed at lower energies for $40° \lesssim \theta_{c.m.} \lesssim 90°$.

[b] The variation is due to the different beam stopping foils used.

[c] Data from Ref. 2 were used along with new data from this work.

not made a serious attempt to measure the isotope distributions at each angle as this would require considerably more beam time. Nevertheless one can get a feeling for these distributions from the results shown in Fig. 5.

The fission-like products as identified by the GT could include contributions from deeply inelastic collisions and nonequilibrium fission as well as from equilibrium fission.[26] It has often been said that for the higher energies and the lower Z targets, this distinction is particularly difficult.[27] In Fig. 4 we show the angular distributions of gross fission-like products (ER and quasielastic products excluded) transformed to c.m. with the assumption that all fragments have the average c.m. velocity of a symmetric fission product.[28] These angular distributions seem to become more asymmetric with increasing beam energy and decreasing Z of target. At forward angles it is especially difficult to distinguish fission products from target-like products of lower Z and the projectile-like products of higher Z. In addition, at back angles the

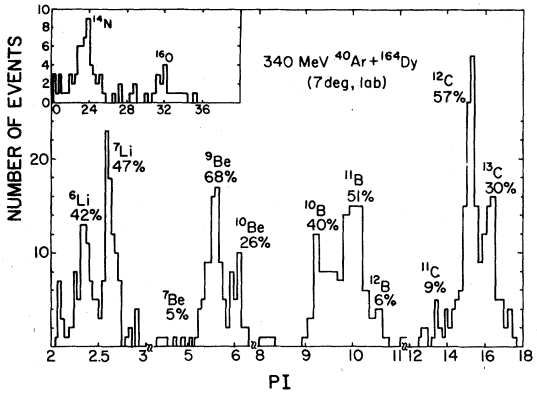

FIG. 5. Example of an isotope distribution of the particles with $3 < Z < 8$. The number of events is plotted versus the value of the "particle identifier function," PI: $PI = [(E_2 + E_1)^{1.73} - E_2^{1.73}]/e_1$. ($E_1$ and E_2 are the energies deposited in the first and second members of the SST; e_1 is the thickness, in μm, of the first detector.) Mass number and percentage occurrence are indicated for each species.

heavier fission products are easily lost below the energy threshold due to the large velocity of the center of mass. However at c.m. angles of ≈90° the energy distributions have a clear valley between broad peaks that one can identify with deeply inelastic and fission reactions. Thus we estimate the fission cross sections to be $2\pi^2(d\sigma/d\Omega)_{90°\text{c.m.}}$ (assuming an angular distribution of $1/\sin\theta_{\text{c.m.}}$) as given in Table III.

Measurements of evaporation residue cross sections were made relative to elastic scattering as they were simultaneously observed in the same GT. The "true" direction of the beam axis was determined by observations of elastic scattering to the right and left sides successively. Rutherford scattering formulas were used for elastic scattering as the angles where ER's were measured are well below the grazing or quarter-point angle. As the recoil energies of heavy residual nuclei after massive transfer are also well above the threshold for GT detection, we would probably include products from most such incomplete fusion reactions as well as those from complete fusion. Therefore the values of ER and fusion cross sections (and the associated values of l_{ER} and l_{crit}) in Table III *should be interpreted as representing complete plus incomplete fusion.*[20] As discussed previously[3] the contribution from incomplete fusion could be very large for reactions induced by 340 MeV ^{40}Ar.

B. Magnitudes of the cross sections

The fusion cross sections of 0.5 to 1.6 b follow the trends of other published data for similar reactions.[3,20,27,29] They imply that very large entrance-channel l waves are involved in the fusing collisions; l_{crit} values range from 65 to 149 (Table III). However, the large cross sections for forward-peaked, light-charged particles (Table II and Fig. 3) also imply significant mixing of complete and incomplete fusion.[2,15-19] Thus the energy and spin values of many heavy nuclei after the fast impact part of the collision may be reduced by several tens of MeV and tens of $\hbar$ units compared to those which would have resulted from complete fusion. Cross sections for the less abundant light charged particles ^{2}H, ^{3}H, Li, Be, B, C, N, and O are also reported in Table II for the 340 MeV ^{40}Ar reactions. As these cross sections are rather small these products probably do not play a major role in the overall mass or energy balance for the reactions. But they may turn out to be useful probes of the role of clustering phenomena in the evolution of the composite system.

The major competitors for the exit channels after equilibration are fission and emission of neutrons, ^{1}H, and ^{4}He. As the evaporative ^{1}H/^{4}He cross sections and decay fractions (Table II and III) seem quite large, it is natural to explore the possibility of evaporation both before and after scission. In another paper[2] we have presented strong arguments against α evaporation from fission fragments for 340 MeV ^{40}Ar + ^{197}Au. Briefly the arguments presented there are as follows: (1) The observed singles spectra are not as wide as those from kinematic simulations of post fission evaporation. (2) The mean energies and the cross sections of ^{4}He are nearly identical in singles and in coincidence at several angles with respect to the fragments. (3) The observed cross section ratios for ^{4}He to ^{1}H are much larger than those expected for evaporation from fission fragments. Each of these arguments also applied for the evaporative ^{1}H, but with much less force. Therefore the possibility remained for some significant evaporation of ^{1}H from the fission fragments.

In this study we have measured the spectra of ^{1}H and ^{4}He in coincidence with one fission product for three geometrical configurations. The shapes of some of these spectra for the ^{154}Sm and ^{116}Sn targets are given in Fig. 6 in comparison to a kinematic calculation. The results for ^{164}Dy are very similar to those for ^{154}Sm. The calculation was made to simulate evaporation from fission fragments with an angular distribution of $1/\sin\theta_{\text{c.m.}}$. The assumed mass, charge, and kinetic energy distributions of the fragments were taken from empirical systematics.[28] All fission fragments were assigned the same multiplicity for light-charged-particle emission (taken to be isotropic).[54]

The evaporation spectrum was assumed to follow Eq. (1) with $T = 2.0$ MeV and barrier parameters from Ref. 7. The energy spectrum for ^{4}He observed in the singles mode is much more narrow than the calculated one. Also the observed spectra for ^{4}He in coincidence are very similar to those in singles and do not exhibit the high-energy peak expected for evaporation from the moving fragments. We conclude that ^{4}He evaporation from the fragments is rare for ^{154}Sm and ^{164}Dy. The data for ^{116}Sn [Fig. 6(b)] allow more room for post fission evaporation, but this is surely not the preferred mechanism. The calculated and observed spectra for ^{1}H in singles at $\theta_{\text{lab}} \approx 104°$ differ only in some details of their shape. However, the observed coincidence spectra exhibit a single peak again very similar to the singles spectrum and qualitatively different from the double-peaked curve expected from two separate fission fragments. We conclude that ^{1}H evaporation for the fission fragments is also rare for ^{154}Sm and ^{164}Dy; similarly for ^{116}Sn this seems not to be the preferred mechanism.

The ratios of evaporative ^{4}He to ^{1}H also provide a test for the extent of post scission emission. This

TABLE III. Summary of ER and fusion cross sections and evaporative decay fractions.

E_{lab} (MeV)	Target [Cpd.sys.]	E^* [a] (MeV)	σ_{ER} (mb)	l_{ER} [b] ($\hbar$)	$\sigma_{fission}$ [c] (mb)	σ_{fusion} (mb)	l_{crit} [d] ($\hbar$)	Cumulative decay fractions [e] ^{1}H	^{2}H	^{3}H	^{4}He	ER	Fission
185		75	538 ± 50	57 ± 3	162 ± 20	700 ± 70	65 ± 3	0.65	0.013	0.004	0.28	0.77	0.23
220	^{116}Sn	102	423 ± 42	55 ± 3	406 ± 41	829 ± 83	77 ± 5	0.76	0.024	0.0045	0.38	0.51	0.49
271	[^{156}Er]	141	335 ± 28	54 ± 2	503 ± 74	838 ± 102	86 ± 6	1.14	0.068	0.021	0.66	0.40	0.60
339		190	416 ± 38	68 ± 3	707 ± 61	1123 ± 100	112 ± 5	1.51	0.14	0.050	1.03	0.37	0.63
221	^{154}Sm	101	86.3 ± 27	26 ± 1.5	754 ± 64	840 ± 74	83 ± 4	0.087	0.008	0.0035	0.092	0.10	0.90
272	[^{194}Hg]	142	79 ± 18	28 ± 1	919 ± 92	998 ± 102	101 ± 6	0.24	0.031	0.016	0.23	0.08	0.92
340		195	124 ± 16	39 ± 2.5	1439 ± 307	1563 ± 323	142 ± 15	0.45	0.069	0.042	0.40	0.08	0.92
221	^{164}Dy	96	13.2 ± 4.2	10 ± 1.6	852 ± 75	875 ± 80	86 ± 4	0.10	0.0055	0.0024	0.064	0.015	0.985
272	[^{204}Po]	137	18.7 ± 6	13 ± 2	949 ± 71	968 ± 77	101 ± 4	0.21	0.025	0.014	0.18	0.019	0.98
339		190	31 ± 6	19 ± 2	1194 ± 207	1225 ± 215	127 ± 11	0.45	0.068	0.038	0.39	0.025	0.975
219	^{197}Au	64			518 ± 46	518 ± 46	68 ± 4	0.061	0.0033	0.0017	0.036		1.0
270	[^{237}Bk]	107			794 ± 142	794 ± 142	94 ± 8	0.13	0.015	0.0097	0.12		1.0
339		161			1577 ± 208	1577 ± 208	149 ± 10	0.24	0.031	0.021	0.23		1.0

[a] Excitation of hypothetical compound nucleus with no rotational energy.
[b] From the equation $\sigma_{ER} = \pi\lambda^2(l_{ER}+1)^2$.
[c] Estimated as described in the discussion of Fig. 4.
[d] From the equation $\sigma_{fusion} = \pi\lambda^2(l_{crit}+1)^2$.
[e] Evaporative H or He or ER or fission cross section divided by the fusion cross section.

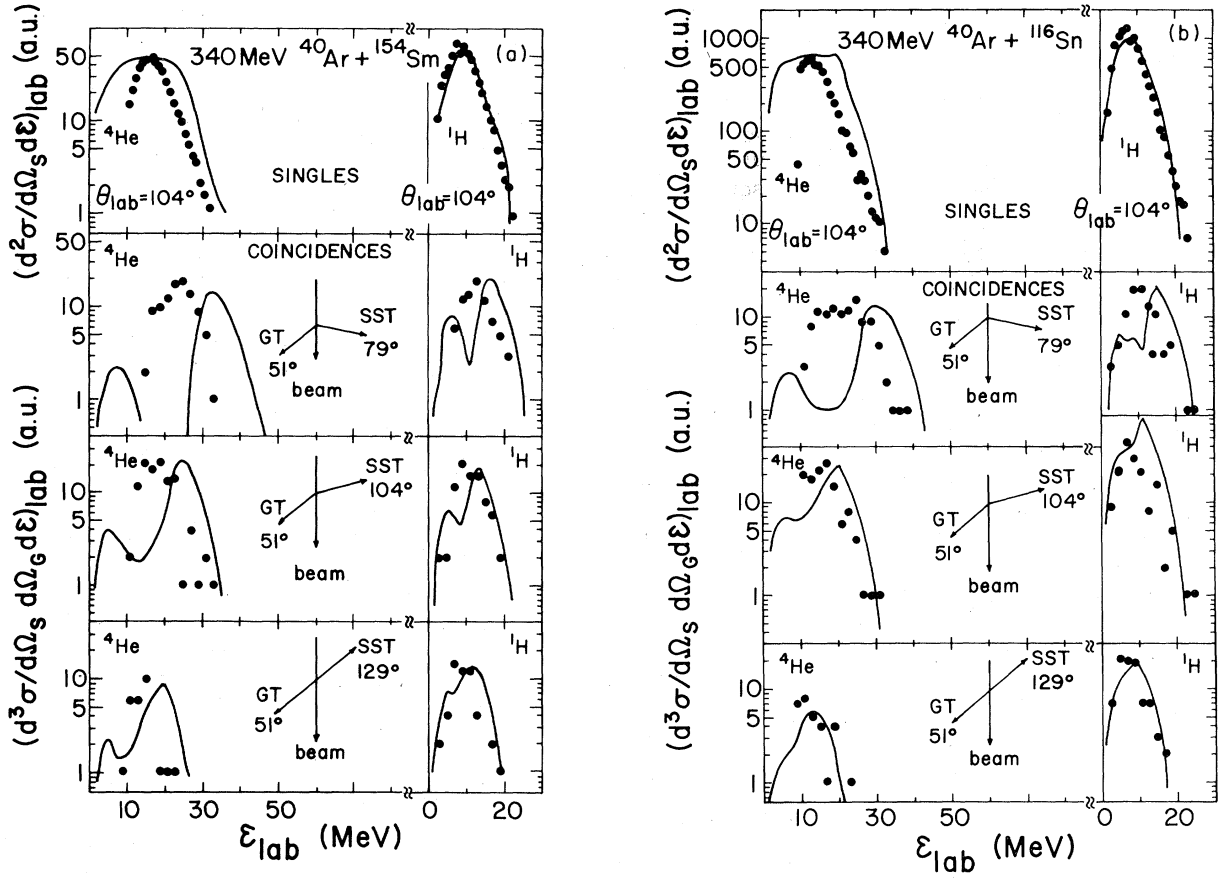

FIG. 6. Spectra for ^{4}He and ^{1}H in singles and in coincidence with one heavy fragment (with the laboratory configuration as shown). The smooth curves were calculated by a Monte Carlo kinematic simulation for evaporation for the fission fragments. (a) ^{40}Ar + ^{154}Sm. (b) ^{40}Ar + ^{116}Sn.

point is discussed more fully in Refs. 2 and 25 so we only mention it here. Examination of Table III shows that the measured ratios of ^{4}He and ^{1}H are all greater than 0.5. (Neglect the data for 222 MeV ^{40}Ar +Sm, Dy, and Au as large uncertainties result from the dominance of the direct component.) Comparison of these ratios to those for the compound nuclei ^{75}Br* or ^{117}Te* would imply implausibly large spins for the fission fragments if they were to be the emission sources.[2,25]

What about evaporation from the fragments after deeply inelastic reactions?[30-34] The H or He evaporated from the rapidly moving and forward-peaked projectile-like product would be included in the group that we call direct. The kinematics is such that H or He evaporated from the slowly moving target-like product could possibly be included with those we assign to the evaporative component. For the similar reaction 373 MeV ^{32}S + ^{197}Au, Gamp *et al.* have made a detailed study of ^{4}He emission in coincidence with projectile-like fragments.[30] They find integrated ^{4}He production in coincidence to be less than 5% of the inclusive cross section. In addition they can exclude emission from the target-like fragment as a prominent mechanism. For 222 and 274 MeV ^{40}Ar reactions the excitation of this target-like fragment is expected to be too low for it to dominate the evaporative H/He. For 340 MeV ^{40}Ar + ^{154}Sm, ^{164}Dy, and ^{197}Au the coincidence data (in Ref. 2 and in this work) indicate that the major (but not exclusive) correlation of coincident events is with fission rather than deeply inelastic reactions. For 340 MeV ^{40}Ar + ^{116}Sn the evaporative ^{1}H/^{4}He cross sections (singles) are so large that contributions are rather likely from several sources: the evaporation residues, the target-like fragments, and the composite systems prior to scission. We will discuss this in connection with Table V later.

C. Anisotropies for H/He and coincidence between fission and ^{1}H and ^{4}He

From Fig. 3 we see that the cross sections for ^{1}H/^{4}He at back angles increase strongly with inci-

dent energy. Also an increase of $d\sigma/d\Omega$ toward 180° becomes apparent at 340 MeV for both ^{4}He and ^{1}H. This back-angle anisotropy is also measurable for ^{4}He for 274 MeV incident energy and for the ^{116}Sn target even at 222 MeV. Anisotropies for the evaporative components are very useful as they can provide information on the root mean square spins of the emitters, $J_{\rm rms}$.[24,25,35] The value of $J_{\rm rms}$ for all fusion reactions is expected to increase with incident energy over the fusion barrier. However, the particular nuclei that evaporate H or He could have $J_{\rm rms}$ values very different from those for all fusion reactions; for example, they could be heavily selected by competition with fission. We have assigned values to the anisotropy parameters β_2 from the fits of Eq. (2) to the data at backward angles (Fig. 3); then we have estimated $J_{\rm rms}$ from these values of β_2.

Catchen *et al.*[25] have discussed the equations from the statistical model that relate these β_2 parameters to the spins of the emitters[24,35]:

$$\beta_2 = \frac{\hbar^2(J_0+\frac{1}{2})^2}{2\mathcal{I}T}\frac{\mu R^2}{\mathcal{I}_\perp}, \tag{4}$$

where J_0 is the spin of the emitting nucleus, $\mathcal{I}$ and T are the moment of inertia and temperature that characterize the level density of the residual nucleus. The exit channel l values are controlled by the centrifugal barrier for particle emission of reduced mass μ [centrifugal barrier $=\hbar^2 l(l+1)/\mu R^2$]. The symbol $\mathcal{I}_\perp$ represents $\mathcal{I}+\mu R^2$. References 7, 10, and 25 use experimental data on fusion and evaporation to examine the choice of parameters $\mathcal{I}$, T, and μR^2 necessary for estimation of $(J_0+\frac{1}{2})^2$ from β_2. Values of β_2 and the associated rms spin $[\langle(J_0+\frac{1}{2})^2\rangle^{1/2}=J_{\rm rms}]$ deduced by their method are also listed in Table IV. See the Appendix for details.

One usually assumes that fission from high-spin nuclei occurs predominantly perpendicular to the spin axis ($K \ll J$).[36] Thus the detection of a fission fragment establishes a reaction plane approximately normal to the spin axis of the fissile nucleus. Particles evaporated prior to fission are expected to have an angular correlation with the spin axis $W(\varphi)$,[24,25]

$$W_{J_0,\mathcal{I}T}(\varphi) \propto \exp(\beta_2 \sin^2\varphi). \tag{5}$$

The determination of β_2 from the angular distribution in singles along with the differential cross section for coincidence between fission and evaporative ^{1}H or ^{4}He ($d^2\sigma/d\Omega_C d\Omega_S$) permits one to integrate and obtain the total cross section for such coincident events.[25] The last two columns in Table IV give the measured differential cross sections and the integrated coincident cross section ($\sigma_{\rm coinc}$). The integrated coincident cross sections have uncertainties of ≈35% due to the statistical significance of the coincidence data and uncertainties in the values of β_2. Nevertheless these estimates can be quite informative as discussed later with Table V. (See the Appendix and Ref. 25 for details of the integration to give $\sigma_{\rm coinc}$.)

IV. DISCUSSION

A. Some simple estimates of the time scales

One of the primary aspects of any reaction mechanism is the relative time scale for the chain of events. Here we consider four kinds of happenings: (1) emission of forward peaked particles H/He, etc., (2) fusion (complete or incomplete), (3) emission of H/He into the backward angles, and (4) fission. The first two must occur in times considerably smaller than a rotation period for the composite system. The latter two are usually thought to require something akin to half a rotation period or even much more. We must resort to some kind of reaction model if we are to set any more stringent limits on these times.

For the forward-peaked H/He we could envisage their prompt ejection after one or a few collisions in much the same picture as the nucleon-nucleon collision model of Serber.[37] Then a typical time would be $\approx R/v$ where a nuclear radius R is taken as a typical traversal distance and v the mean velocity during the traversal. For nucleons one would estimate v to be of the order of the Fermi velocity; for heavier particles (^{4}He, etc.) the whole notion of the Serber model seems rather unnatural. Nevertheless such a picture should lead to $\approx 1\times10^{-22}$ sec for a nuclear traversal time in a collision cascade model.

One might argue that the colliding nuclei must move toward one another for some significant distance (e.g., $\frac{1}{2}R$) in order to provide the initial collisions needed to cut away the light-charged particles from their sisters.[38] Hence another $2-3\times10^{-22}$ sec would be a reasonable mean induction time for a collision cascade model.

The hot-spot model provides another simple means to estimate an upper limit for the mean decay time.[6,39] One can visualize a small hot zone on the nuclear surface that emits a narrow beam of particles. Then the mean decay time is given by the mean decay angle divided by the angular velocity ω. The former can be taken from the data in Fig. 3 (for T vs $\theta_{\rm c.m.}$) after subtracting an assumed symmetric component. The angular velocity can be obtained if one can estimate a mean l value and a moment of inertia. From reactions induced by lighter projectiles, gamma ray data in coincidence with forward-peaked ^{4}He seem to indicate that the value of $l_{\rm crit}$ is probably near to the relevant mean

TABLE IV. Summary of anisotropy parameters, J_{rms} for the emitters and integrated coincidence cross sections (evaporative component).

E_{lab} (MeV)	Target	β_2 [a]	J_{rms} [b] ($\hbar$)	$d^2\sigma/d\Omega_G d\Omega_S$ [c] (mb/sr^2)	σ_{coinc} [d] (mb)
			^{4}He		
220	^{116}Sn	1.49 ± 0.57 [e]	52 ± 12 [e]		
271	^{116}Sn	1.98 ± 1.03	65 ± 17		
339	^{116}Sn	1.70 ± 0.70	66 ± 13	3.50	232 ± 82 [f]
272	^{154}Sm	1.58 ± 0.84	74 ± 17		
340	^{154}Sm	1.89 ± 0.55	89 ± 13	4.3	287 ± 94
272	^{164}Dy	1.33 ± 0.62	73 ± 16		
339	^{164}Dy	1.05 ± 0.57	72 ± 27	4.4	406 ± 48
270	^{197}Au	0.28 ± 0.28	38^{+19}_{-38}		
339	^{197}Au	1.11 ± 0.58	82 ± 20	2.8 [g]	252 [g]
			^{1}H		
339	^{116}Sn	0.95 ± 0.82	97 ± 40	4.4	356 ± 85
340	^{154}Sm	0.78 ± 0.39	115 ± 20	4.0	348 ± 49
272	^{164}Dy	0.19 ± 0.19	60^{+30}_{-60}		
339	^{164}Dy			3.0	346 ± 39
339	^{197}Au	0.98 ± 0.69	140 ± 40	1.6 [g]	145 [g]
			^{2}H		
220	^{116}Sn	1.48 ± 0.65	67 ± 14		
271	^{116}Sn	1.89 ± 1.11	82 ± 20		
339	^{116}Sn	2.50		0.55	34 ± 17
340	^{154}Sm	1.04 ± 0.42	92 ± 18	0.85	71 ± 20
339	^{164}Dy	0.50 ± 0.45	70 ± 31	0.54	53 ± 24
339	^{197}Au	1.49 ± 1.00	124 ± 35		
			^{3}H		
339	^{116}Sn	2.88		0.20	11.3 ± 2.3
272	^{154}Sm	0.76 ± 0.51	55 ± 18		
340	^{154}Sm	0.97 ± 0.42	68 ± 14	0.28	24 ± 16
339	^{164}Dy	0.75 ± 0.51	64 ± 20	0.32	29 ± 25
339	^{197}Au	0.76 ± 0.76	72 ± 36		

[a] From fits of Eq. (2) to data in Fig. 3.
[b] See discussion of Eq. (4) and Ref. 25 for tests of the parameters used.
[c] The average of the c.m. cross sections observed for the three configurations in Fig. 6.
[d] From the integration of Eq. 5 as described in the Appendix and in Ref. 25.
[e] Uncertainties estimated from maximum and minimum values of β_2 that give an acceptable fit (by eye) to the data in Fig. 3.
[f] Uncertainty from reproducibility of $d^2\sigma/d\Omega_G d\Omega_S$ only.
[g] Data from Ref. 2, normalized to singles data from this work by the factor 0.71.

l value.[16-19] A configuration of two touching spheres probably provides a reasonable estimate of the relevant moment of inertia (possibly this should be considered as an upper limit). Mean decay times so estimated are $\approx 3-8\times10^{-22}$ sec. The precision of the data in Fig. 3 and the crudely estimated values of $\mathcal{I}$ and ω preclude any discussion of Z or energy dependence of these times. The important point is simply their very small values $5\pm3\times10^{-22}$ sec. (These times may even be overestimated by our parameter choices and the model of a narrow emission cone from the hot-spot zone. For example a smaller moment of inertia would give even shorter times.)

It is interesting that the mean times from the hot-spot and traversal models are so similar. The implication is that the emissions occur so rapidly that rather little rotation of the composite system occurs; hence an essential distinction between the two models is nearly removed for the forward-peaked component. Also interesting is the implication that these forward-peaked particles are ejected so rapidly that the fusion decision is yet to be made.[3] For entrance channel l values near to or less than l_{crit} most fusion models[10-14] visualize the partners approaching one another with a very small radial velocity. Thus the traversal of the real potential barrier toward fusion is explored

TABLE V. Flow chart for singles and coincidence cross sections (mb) for 340 MeV ^{40}Ar+X. [a]

	^{116}Sn		^{154}Sm		^{164}Dy		^{197}Au	
$\sigma_R(l_{max})$	2483	(168)	2565	(180)	2530	(179)	2407	(180)
$\sigma_{QE}+\sigma_{DI}$	1360		1002		1305		830	
Direct	495 (^{4}He) 97 (^{2,3}H)	466 (^{1}H) 15 (Li–O)	566 (^{4}He) 113 (^{2,3}H)	392 (^{1}H) 24 (Li–O)	386 (^{4}He) 71 (^{2,3}H)	251 (^{1}H) 16 (Li–O)	204 (^{4}He) 42 (^{2,3}H)	127 (^{1}H) 7 (Li–O)
$\sigma_{CF}(l_{crit})$	1123	(112)	1563	(142)	1225	(127)	1577	(149)
Evaporative (J_{rms})	1158 (^{4}He) (66)	1697 (^{1}H) (100)	624 (^{4}He) (89)	703 (^{1}H) (115)	478 (^{4}He) (72)	553 (^{1}H)	359 (^{4}He) (82)	386 (^{1}H) (140)
Evaporative in coincidence with fission	232 (^{4}He)	356 (^{1}H)	287 (^{4}He)	348 (^{1}H)	406 (^{4}He)	346 (^{1}H)	252 [a] (^{4}He)	145 [a] (^{1}H)
Fission	707		1439		1194		1577	
Evaporative but not in coincidence with fission	926 (^{4}He)	1341 (^{1}H)	337 (^{4}He)	355 (^{1}H)	72 (^{4}He)	207 (^{1}H)	107 [a] (^{4}He)	241 [a] (^{1}H)
$\sigma_{ER}(l_{ER})$	416	(68)	124	(39)	31	(19)	0	(0)

[a] These results include additional and updated results compared to those reported at the International Conference on Continuum Spectra, San Antonio, Texas, 1979.

with this slow radial motion, and the time for the double nuclear system to rotate ≈1 rad may give a rough estimate of the time to decide for or against fusion. For these systems rotation through 1 rad (for touching spheres at l_{crit}) requires $6-20\times10^{-22}$ sec. We conclude that the ejection of forward-peaked H/He (for $l\approx l_{crit}$) probably occurs concurrently with or prior to the fusion decision and should be allowed for in a useful reaction model.[3] This point is addressed in an extension of the sharp cutoff classification by Siwek-Wilczyńska *et al.*,[18] but not in the models that focus on an *a priori* potential.[10-14]

The apparently slower decay modes, H/He evaporation and fission, also provide an interesting insight into the relative decay times. The values of l_{crit} for 340 MeV ^{40}Ar reactions (109–145 $\hbar$) are considerably larger than the calculated stability limits in the liquid drop model (≈80 $\hbar$). Several authors have proposed the transient stability of a double-nucleus system for $\approx1\times10^{-21}$ sec.[26] Such an entity could indeed be responsible for the large observed values of l_{crit}. It is especially interesting that evaporative H/He emission precedes the scission of even such short lived species. Extensive energy mixing and evaporative decay must occur on a time scale comparable to scission. This implication of extremely rapid energy thermalization is encouraging for diffusion models that have assumed thermal equilibration at each step in deeply inelastic reactions.[40]

B. The charge and energy dependence of various processes

In Fig. 7 we show the Z dependence of the cross sections for each process we study at three excitation energies for the compound nucleus. The fusion cross sections are rather insensitive to Z for each energy; by contrast the fraction of ER decreases by more than tenfold from $Z=68$ to 84 and by much more from $Z=84$ to 97. This decrease is generally attributed to a decreasing fission barrier[41] which rapidly increases the number of available channels to fission. As the direct H and He are expected to be emitted before equilibration they should not be affected by the number of available fission channels and indeed they are relatively constant with Z (e.g., ≈100 mb at $E^*=100$ MeV, 100–250 mb at 140 MeV, and 150–500 mb at 190 MeV).

On the other hand if the low-temperature H and He are evaporated from a completely equilibrated compound nucleus, then their abundance (Fig. 7) and the values of J_{rms} for the emitters (Table IV) should reflect the Z and J dependence of the fission barrier. The expected decrease in cross section is indeed observed from $Z=52$ to 68 to 80. However, for $Z=80$ to 84 and even 97 there is scarcely any change. (Recall that in Sec. III B we showed that there is very little H/He emission from fragments after scission.) These low-temperature H/He emissions seem to precede scission and are characterized by $J_{rms}\approx 50-100\,\hbar$ (or $\approx l_{crit}$/

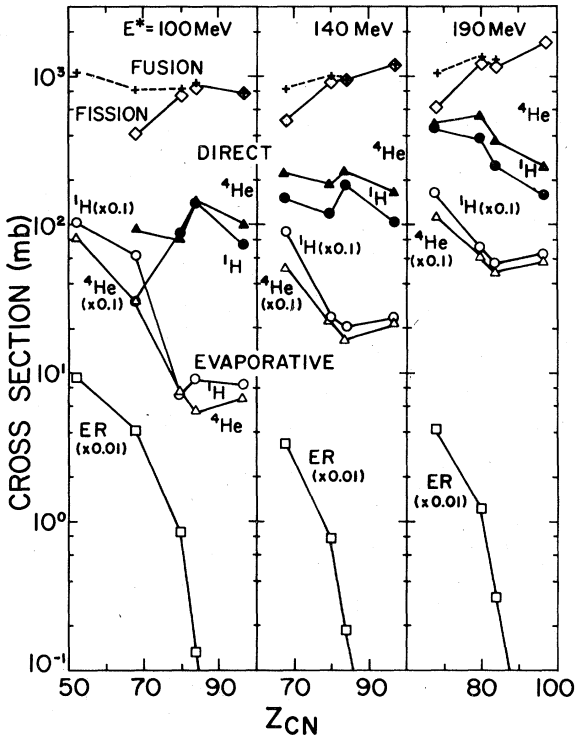

FIG. 7. Integrated cross sections at three excitation energies for fusion, fission, ^{4}He, ^{1}H, and ER vs charge of the composite nucleus, Z_{CN}. Data for a target of ^{77}Se are from Ref. 8. Data for ^{116}Sn, ^{154}Sm, and ^{164}Dy were taken directly from the measurements; those for ^{197}Au were interpolated and extrapolated to the indicated excitation energies (see Table III).

$\sqrt{2}$) regardless of Z and the number of open fission channels. The rapid increase of these evaporative emissions with energy (Fig. 7 and the cumulative decay fractions in Table III) suggests that they become exit channels of major importance. This is not easy to rationalize with a standard statistical model that utilizes similar energy dependence for the level density of saddle-point and evaporation daughter nuclei.[21] We conclude that the dynamics of the intrinsic rates of the emission processes control their abundance relative to fission rather than the available phase space. The scission time has been estimated to be $\gtrsim 3\times10^{-21}$ sec[42] whereas the time for thermal equilibration and subsequent evaporation[43] seems to be even shorter (or at least comparable). This we feel is a very important result as it implies that the H/He spectra might give a running record of the extent of the thermalization processes before scission. It also implies that the sharp-cutoff approximation for fission evaporation competition [$\Gamma_f/\Gamma_{tot} \to 1$ for $J > J_f$ where $B_f(J_f) = B_n$] is simply not valid for high excitation energies.[44] We discuss this point more fully in Ref. 4.

There are several additional important implications of a shift from control by phase space to control by dynamics. Our equations based on equilibrium statistical mechanics surely lose their generality, and the regal position of the fission saddle point is threatened. Evaporation of H or He could conceivably occur either before or after traversal of the saddle point as discussed above. But also the fissile system may not have enough time to explore all its K states as assumed in an equilibrium model.[36] Such a situation would severely shake the foundations used for exploring angular momentum transfer via sequential fission studies.[45,46] Recent results from the Heidelberg group[46] do indeed suggest the demise of equilibrium theory for the angular correlations observed for sequential fission in the reactions ^{238}U + ^{238}U and ^{238}U + ^{248}Cm.

An additional consequence of a shift to dynamic control is the possibility of invalidation of the Bohr independence hypothesis for the excited "compound" nuclei.[47] "Fission" probability could depend on mass asymmetry of the collision partners in addition to spin and excitation energy.[26,48] As the limits for complete equilibrium are approached and passed it is likely that some decay modes will retain the features of equilibration longer than others.[49] The angular distributions and temperatures shown in Fig. 3 suggest that H and He emission at backward angles may be clinging tenaciously to their evaporative character. However, the collective motion toward fission may well be too slow to explore all the open channels that are available.

The forward-peaked emission of the various light particles clearly does not originate from evaporation. From Table II we see that there is relatively little dependence of these cross sections on target Z. Also it is interesting that one observes so much of the loosely bound ^{2}H and ^{3}H and even the more complex ions Li, Be, B, C, N, and O. It would seem likely that such particles would be ejected either at impact or at scission.[50] The similarity of their angular distributions to those for protons could be said to suggest similarity in their mechanistic origin. This reasoning argues against reaction models which employ long mean free paths inside the nucleus.[11,51]

C. A flow chart to summarize our findings for 340 MeV ^{40}Ar + ^{116}Sn, ^{154}Sm, ^{164}Dy, and ^{197}Au

In Table V we present a summary of many of the cross sections and spin values that we have taken from experimental observations or systematics. Let us follow down the column for the target ^{116}Sn. From systematics of elastic scattering data one

estimates a reaction cross section (σ_R) of 2483 mb and $l_{max}=168$.[52] Subtraction of the measured fission and ER cross section leads to 1436 mb for quasielastic and deeply inelastic reactions ($\sigma_{QE}+\sigma_{DI}$). Direct (or forward-peaked) emission of light-charged particles gives a comparable sum, some of which surely accompanies the so-called "fusion" cross section (σ_{CF}) and complicates its common designation "complete fusion". The evaporative cross sections for ^{4}He and ^{1}H are as large or larger than the fusion cross sections and values of J_{rms} (from the angular distributions) are very similar to $l_{crit}/\sqrt{2}$. This result is consistent with a constant probability of emission from entrance channel waves of $0<l\lesssim l_{crit}$. Normally one expects fission competition to eliminate the evaporative emission from the higher spin states. For the Sn target about one fourth of the evaporative ^{4}He and ^{1}H (232 and 356 mb) are found in coincidence with fission. Presumably most of the rest (926 mb ^{4}He and 1341 mb ^{1}H) comes from the ER products. The implied charge loss for the ER products ($\Delta Z\approx 7$ units) is consistent with that observed by other workers.[44] The observed cross sections for evaporative ^{4}He and ^{1}H in coincidence with fission are about the same for all targets in spite of the very large difference in fissionabilities. One possible interpretation of this result is that the time for motion to the scission point is sufficiently long to allow essentially complete energy thermalization and a rate determined evaporation probability of $\approx\frac{1}{3}$ to $\frac{1}{2}$ for ^{1}H or ^{4}He. By contrast, the evaporative ^{4}He not in coincidence with fission decreases rapidly with Z following the decrease in evaporation residues. Possibly this result reflects rather constant values of Γ_α/Γ_n for each of the evaporation chains. The corresponding Z dependence for evaporative ^{1}H not in coincidence with fission is not as strong with apparently ≈200 mb remaining even for Dy and Au targets. Presumably these protons were evaporated from target-like products after deeply inelastic reactions. More extensive coincidence measurements are required to explore this point.

D. Suggestions for further experimentation

It is very interesting that the direct component of the charged-particle emission seems to be emitted so rapidly that very little rotation of the composite system can occur. If a "hot spot" is formed[39] and emission occurs at the touching points one would expect a decided energy dependence of the angular distribution. At near barrier energies one would expect the grazing angle to move aft, and along with it the direct emission of H/He to move away from zero degrees. Such a change is not apparent in Fig. 3, but one should make measurements at still lower energies to force a large increase in the angle for the grazing collisions. If the direct emission becomes more forward peaked at near barrier energies than at higher energies one might infer that high velocity particles traverse the nucleus similar to the "promptly emitted particle" mechanism.[51] In that case the source of cluster emission (e.g., ^{2}H, ^{3}H, ^{4}He, ...) is both very puzzling and interesting. The similarity of the angular distributions for protons and all the other light-charged particles is consistent with a single mechanism for their production.

For the evaporative H/He emission it would be very interesting to obtain more extensive coincidence data (with fission,[1,2] deeply inelastic reactions,[30-34] and with specific residual nuclei[19] after evaporation). This could allow much more detail in the discussion of the angular momentum deposition for individual exit channels. Experimentation in both of these directions has been undertaken.

V. SUMMARY

We have presented a systematic pattern for light-charged particle emission, fission, and ER production in several ^{40}Ar reactions. The spectra and angular distributions of H/He are consistent with a low-temperature evaporative component at back angles and a high-temperature direct component at forward angles. Forward-peaked emission of Li, Be, B, C, N, and O was also observed for 340 MeV ^{40}Ar. Fission-like products were observed with a gas ionization detector; their angular distributions approach $1/\sin\theta_{c.m.}$ for the ^{197}Au target, but become forward-peaked for lighter targets. Energy spectra and cross sections measured in both singles and coincidence modes indicate H/He emission prior to scission.[2] From the anisotropies in the backward hemisphere one can estimate the rms spin of the emitting nuclei to be ≈50–100. Coincidence measurements for 340 MeV ^{40}Ar show that 200–400 mb of evaporative ^{1}H and ^{4}He are emitted in coincidence with fission for all four targets. The large amount of evaporation in competition with fission is difficult to explain with phase-space models. The large amount of forward-peaked light-charged particles implies significant energy dissipation concurrent with the fast impact period of $\approx 5\times10^{-22}$ sec. The presence of a significant number of complex particles ^{2}H, ^{3}H, Li, ... provides a probe of nucleonic clustering in the very early life of the composite nucleus.

ACKNOWLEDGMENTS

This work was supported in part by the Division of Nuclear Physics of the U. S. Department of

Energy and by CNRS of France. The staff of the SuperHILAC accelerator at the Lawrence Berkeley Laboratory has been very helpful. We have especially appreciated the data acquisition program written by Creve Maples and the consideration extended to us by R. Stevenson.

APPENDIX

In order to obtain an integrated cross section σ_{coinc} for a light particle (L) in coincidence with a heavy fission fragment (H) we must adopt a reaction model and its associated angular distributions. We use the equilibrium statistical model for evaporation of the light-charged particle[24] followed by fission in a plane perpendicular to the spin vector. Our detection of the fission fragment then fixes a reaction plane and the spin of the composite system perpendicular to it. In Ref. 25 the expected angular correlations with respect to the spin vectors were discussed. Here we restate the equation used and the choice of parameters as taken from that study.[25] The angular correlation of particle L with respect to this spin vector is $W_{J_0,\mathcal{I}T}(\varphi)$ as given by Eq. (5). Its integration over the directions of the light particle gives $(d\sigma_L/d\Omega_H)$

$$d\sigma_L/d\Omega_H = 4\pi \int_0^{\pi/2} W(\varphi)\sin\varphi d\varphi$$

$$= 2\pi W(90°)(\pi/\beta_2)^{1/2}\,\mathrm{erf}(\beta_2{}^{1/2}), \qquad (6)$$

where $W(90°)$ is the in plane coincidence cross section $d\sigma_L{}^2/d\Omega_L d\Omega_H$. Then the integration over all fission fragment directions is made with the assumption of c.m. angular distribution proportional to $1/\sin\theta_H$. We have used values of β_2 determined by fits to the angular distribution as measured in singles (see Table IV). To the extent that fission selects a high-spin fraction of these events we underestimate β_2. To the extent that our model ignores misalignment of the spin vector from the normal to the reaction plane,[36] we overestimate the effective value of β_2.

From Eq. (4) it is clear that if one seeks to estimate $\langle(J_0+\frac{1}{2})^2\rangle^{1/2}$ from the measured value of β_2 then he must assign numerical values to $\mathcal{I}$, T, and μR^2. We have taken the value of μR^2 from empirical studies[7] of fusion of ^{4}He and ^{1}H,

$$\mu R^2 = \mu(1.42A^{1/3} + R_p \text{ or } R_\alpha)^2, \qquad (7)$$

with $R_p = 1.44$ fm and $R_\alpha = 2.53$ fm. The moment of inertia $\mathcal{I}$ was taken to be that of a rigid sphere of radius $1.20A^{1/3}$ fm. The temperature is related to the average energy available for thermal excitation:

$$U = aT^2, \qquad (8)$$

with "a" $= (A/10)$ MeV^{-1} and

$$U = E^* - \langle\epsilon\rangle - S - E_{\text{rot}}. \qquad (9)$$

The separation energy of the emitted particle is S and its average kinetic energy is $\langle\epsilon\rangle$,

$$\langle\epsilon\rangle \approx B + 2T. \qquad (10)$$

In Ref. 25 a detailed comparison is made of measured values of β_2 to values calculated by this parametrization, using available data for ^{75}Br* and ^{117}Te*.[8,53]

---

*Permanent address: Centre d'Etudes Nucléaires de Bordeaux-Gradignan, Laboratoire de Chimie Nucléaire ERA No. 144, Le Haut Vigneau, 33170 Gradignan, France.

†Permanent address: Laboratoire de Chimie Nucléaire, Institut de Physique Nucléaire, B.P. No. 1, 91406 Orsay, France.

[1] J. M. Miller, D. Logan, G. L. Catchen, M. Rajagopalan, J. M. Alexander, M. Kaplan, J. W. Ball, M. S. Zisman, and L. Kowalski, Phys. Rev. Lett. 40, 1074 (1978).

[2] D. Logan, M. Rajagopalan, M. S. Zisman, J. M. Alexander, M. Kaplan, and L. Kowalski, Phys. Rev. C 22, 104 (1980).

[3] H. Delagrange, D. Logan, M. F. Rivet, M. Rajagopalan, J. M. Alexander, M. S. Zisman, M. Kaplan, and J. W. Ball, Phys. Rev. Lett. 43, 1490 (1979).

[4] M. Rajagopalan, D. Logan, J. W. Ball, M. Kaplan, H. Delagrange, M. F. Rivet, J. M. Alexander, and M. S. Zisman (unpublished).

[5] H. C. Britt and A. R. Quinton, Phys. Rev. 124, 877 (1961).

[6] T. Nomura, H. Utsunomiya, T. Motobayashi, T. Inamura, and M. Yanokura, Phys. Rev. Lett. 40, 694 (1978).

[7] M. A. McMahan and J. M. Alexander, Phys. Rev. C 21, 1261 (1980).

[8] J. Galin, B. Gatty, D. Guerreau, C. Rousset, U. C. Schlotthauer-Voos, and X. Tarrago, Phys. Rev. C 9, 1113, 1126 (1974); 10, 638 (1974).

[9] W. U. Schröder and J. R. Huizenga, Annu. Rev. Nucl. Sci. 27, 465 (1977).

[10] L. C. Vaz and J. M. Alexander, Phys. Rev. C 18, 2152 (1978); L. C. Vaz, J. M. Alexander, and G. R. Satchler (unpublished).

[11] J. R. Birkelund and J. R. Huizenga, in Proceedings of the Symposium on Heavy-Ion Elastic Scattering, Rochester, New York, 1977 (unpublished); J. R. Birkelund, J. R. Huizenga, J. N. De, and D. Sperber, Phys. Rev. Lett. 40, 1123 (1978); J. R. Birkelund, L. E. Tubbs, J. R. Huizenga, J. N. De, and D. Sperber, Phys. Rep. C 56, 107 (1979).

[12] J. Galin, D. Guerreau, M. Lefort, and X. Tarrago, Phys. Rev. C 9, 1018 (1974); C. Ngô, B. Tamain,

J. Galin, M. Beiner, and R. J. Lombard, Nucl. Phys. A240, 353 (1975).
[13]K. Siwek-Wilczyńska and J. Wilczyński, Phys. Lett. 74B, 313 (1978).
[14]B. Sikora, M. Blann, W. Scobel, J. Bisplinghoff, and M. Beckerman, Phys. Rev. C 21, 614 (1980).
[15]R. Bimbot, D. Gardès, and M. F. Rivet, Nucl. Phys. A189, 193 (1972).
[16]T. Inamura, M. Ishihara, T. Fukuda, and T. Shimoda, Phys. Lett. 68B, 51 (1977).
[17]D. R. Zolnowski, H. Yamada, S. E. Cala, A. C. Kahler, and T. T. Sugihara, Phys. Rev. Lett. 41, 92 (1978); H. Yamada, D. R. Zolnowski, S. E. Cala, A. C. Kahler, J. Pierce, and T. T. Sugihara, *ibid.* 43, 605 (1979).
[18]K. Siwek-Wilczyńska, E. H. duMarchie van Voorthuysen, J. van Popta, R. H. Siemssen, and J. Wilczyński, Phys. Rev. Lett. 42, 1599 (1979).
[19]D. G. Sarantites, L. Westerberg, M. L. Halbert, R. A. Dayras, D. C. Hensley, and J. H. Barker, Phys. Rev. C 18, 774 (1978); K. A. Geoffroy, D. G. Sarantites, M. L. Halbert, D. C. Hensley, R. A. Dayras, and J. H. Barker, Phys. Rev. Lett. 43, 1303 (1979).
[20]See for example, M. Lefort, J. Phys. (Paris) C5, 57 (1976).
[21]H. Delagrange, A. Fleury, and J. M. Alexander, Phys. Rev. C 16, 706 (1977).
[22]E. Baron, Ph.D thesis, University of Paris, Orsay, France (1975) (unpublished); E. Baron and B. Delaunay, Phys. Rev. A 12, 40 (1975).
[23]M. M. Fowler and R. C. Jared, Nucl. Instrum. Methods 124, 341 (1975).
[24]T. Døssing (unpublished).
[25]G. L. Catchen, M. Kaplan, J. M. Alexander, and M. F. Rivet, Phys. Rev. C 21, 940 (1980).
[26]W. Nörenberg and C. Riedel, Z. Phys. A 290, 335 (1979); G. J. Mathews and L. G. Moretto, Phys. Lett. 87B, 331 (1979); C. Grégoire, R. Lucas, C. Ngô, and B. Schürmann, Saclay Report No. DPH-N/MF/79/33 (unpublished).
[27]See, for example, H. C. Britt, B. H. Erkkila, R. H. Stokes, H. H. Gutbrod, F. Plasil, R. L. Ferguson, and M. Blann, Phys. Rev. C 13, 1483 (1976).
[28]E. K. Hyde, *The Nuclear Properties of the Heavy Elements* III, *Fission Phenomena* (Prentice-Hall, Englewood Cliff, N.J., 1964); V. E. Viola, Jr., Nucl. Data A1, 391 (1966).
[29]S. Della Negra, H. Gauvin, H. Jungclas, Y. Le Beyec, and M. Lefort, Z. Phys. A 282, 65 (1977); N. H. Lu, D. Logan, J. M. Miller, T. W. Debiak, and L. Kowalski, Phys. Rev. C 13, 1496 (1976); W. Scobel, H. H. Gutbrod, M. Blann, and A. Mignerey, *ibid.* 14, 1808 (1976); H. Gauvin, D. Guerreau, Y. Le Beyec, M. Lefort, F. Plasil, and X. Tarrago, Phys. Lett. 58B, 163 (1975); B. Tamain, C. Ngô, J. Péter, and F. Hanappe, Nucl. Phys. A252, 187 (1975); C. Ngô, J. Peter, B. Tamain, M. Berlanger, and F. Hanappe, Z. Phys. A 283, 161 (1977).
[30]A. Gamp, J. C. Jacmart, N. Poffé, H. Doubre, J. C. Roynette, and J. Wilczyński, Phys. Lett. 74B, 215 (1978); A. Gamp, H. L. Harney, J. C. Roynette, E. Plagnol, H. Fuchs, H. Doubre, J. C. Jacmart, and N. Poffé, Z. Phys. A 291, 347 (1979).
[31]J. M. Miller, G. L. Catchen, D. Logan, M. Rajagopalan, J. M. Alexander, M. Kaplan, and M. S. Zisman, Phys. Rev. Lett. 40, 100 (1978); and unpublished data.
[32]J. W. Harris, T. M. Cormier, D. F. Geesaman, L. L. Lee, Jr., R. L. McGrath, and J. P. Wurm, Phys. Rev. Lett. 38, 1460 (1977).
[33]R. Albrecht, W. Dünnweber, G. Graw, H. Ho, S. G. Steadman, and J. P. Wurm, Phys. Rev. Lett. 34, 1400 (1975); H. Ho, R. Albrecht, W. Dünnweber, G. Graw, S. G. Steadman, J. P. Wurm, D. Disdier, V. Rauch, and F. Scheibling, Z. Phys. A 283, 235 (1977).
[34]C. K. Gelbke, M. Bini, C. Olmer, D. L. Hendrie, J. L. Laville, J. Mahoney, M. C. Mermaz, D. K. Scott, and H. H. Wieman, Phys. Lett. 71B, 83 (1977).
[35]T. Ericson and V. Strutinsky, Nucl. Phys. 8, 284 (1958); 9, 689 (1959).
[36]R. Vandenbosch and J. R. Huizenga, *Nuclear Fission* (Academic, New York, 1973).
[37]R. Serber, Phys. Rev. 72, 1114 (1947); Y. Yariv and Z. Fraenkel, Phys. Rev. C 20, 2227 (1979).
[38]M. Blann, Nucl. Phys. A235, 211 (1974); M. Blann, A. Mignerey, and W. Scobel, Nukleonika 21, 335 (1976).
[39]R. M. Weiner and M. Weström, Phys. Rev. Lett. 34, 1523 (1975).
[40]The importance of the various relevant time scales is discussed by D. Agassi, C. M. Ko, and H. A. Weidenmüller, Ann. Phys. (N.Y.) 107, 140 (1977) and (unpublished).
[41]S. Cohen, F. Plasil, and W. J. Swiatecki, Ann. Phys. (N.Y.) 82, 557 (1974).
[42]J. R. Nix, Argonne National Laboratory Report No. ANL-PHY-76-2, Vol. I, (1976).
[43]A. Fleury, H. Delagrange and J. P. Dufour, Phys. Rev. C 16, 1396 (1977).
[44]The sharp cutoff approximation is often used as a guide. See for example Ref. 22 and H. C. Britt, B. H. Erkkila, P. D. Goldstone, R. H. Stokes, B. B. Back, F. Folkmann, O. Christensen, B. Fernandez, J. D. Garrett, G. B. Hagemann, B. Herskind, D. L. Hillis, F. Plasil, R. L. Ferguson, M. Blann, and H. H. Gutbrod, Phys. Rev. Lett. 39, 1458 (1977); A. Gavron, Phys. Rev. C 21, 230 (1980).
[45]P. Dyer, R. J. Puigh, R. Vandenbosch, T. D. Thomas, and M. S. Zisman, Phys. Rev. Lett. 39, 392 (1977).
[46]D. v. Harrach, P. Glässel, Y. Civelekoglu, R. Männer, and H. J. Specht, Phys. Rev. Lett. 42, 1728 (1979); D. v. Harrach, P. Glässel, Y. Civelekoglu, R. Männer, H. J. Specht, J. B. Wilhelmy, H. Freiesleben, and K. D. Hildenbrand, International Symposium on Physics and Chemistry of Fission, Jülich, Germany, 1979, (paper IAEA-SM-241/D4).
[47]N. Bohr, Science 86, 161 (1937).
[48]S. Agarwal, Ph.D thesis, University of Paris, Orsay, France (1980) (unpublished).
[49]L. G. Moretto, J. Galin, R. Babinet, Z. Fraenkel, R. Schmitt, R. Jared, and S. G. Thompson, Nucl. Phys. A259, 173 (1976).
[50]I. Halpern, Ann. Rev. Nucl. Sci. 21, 245 (1971).
[51]J. P. Bondorf, J. N. De, A. O. T. Karvinen, G. Fai, and B. Jakobsson, Phys. Lett. 84B, 162 (1979).
[52]L. C. Vaz and J. M. Alexander, Phys. Rev. C 18, 833 (1978); J. M. Alexander, H. Delagrange, and A. Fleury, Phys. Rev. C 12, 149 (1975).
[53]R. C. Reedy, M. J. Fluss, G. F. Herzog, L. Kowalski, and J. M. Miller, Phys. Rev. 188, 1771 (1969).
[54]Recently γ ray multiplicities have been measured for several fission reactions induced by heavy ions, e.g.,

$^{16}O + ^{208}Pb$ and ^{181}Ta, J. W. Ball, A. F. Dalmanian, S. Gazes, A. P. Smith, S. G. Steadman, F. Videbaek, G. R. Young, private communication; J. W. Ball, S. G. Steadman, L. Grodzins, F. Videbaek, and G. R. Young, Bull. Am. Phys. Soc. 24, 696 (1979). Typically the γ ray multiplicities are ≈ 8 per fission event which indicates that only a small fraction of the spin of the fissile nucleus is converted into the spins of the fission fragments. The oft-used sticking model also implies only small spins on the fission fragments. With these considerations we feel that isotropy is a good approximation to the angular distribution expected for H/He evaporation from fission fragments.